Ultrawide-Band Photonic Time-Stretch A/D Converter Employing Phase Diversity

Yan Han, *Member, IEEE*, Ozdal Boyraz, and Bahram Jalali, *Fellow, IEEE*

Abstract—The performance of analog-to-digital converters can be greatly enhanced by preprocessing the analog signal using the photonic time-stretch technique. The analog bandwidth of a time-stretch preprocessor is limited by dispersion-induced frequency fading. In this paper, we propose and demonstrate a new implementation of the time-stretch analog-to-digital (A/D) conversion system that overcomes the bandwidth limitation. It is shown that the fading phenomenon can be mitigated by using phase diversity, and the maximum ratio combining algorithm is identified as a potential technique for maximizing the signal-to-noise-ratio. Real-time A/D conversion at 480 Gsample/s is demonstrated.

Index Terms—Fiber optics, microwave photonics, optical signal processing, photonic analog-to-digital (A/D) conversion, time stretch.

I. INTRODUCTION

IN RADAR and communication systems, the use of digital signal processing offers higher performance and fast system reconfigurability. Typically, the analog-to-digital converter (ADC) is the major bottleneck in realizing such systems as the stringent sampling rate and input bandwidth requirements are beyond what is available from state-of-art electronic digitizers. Faster ADCs are also needed for the single-shot real-time measurement of ultrawide-band waveforms. Various photonic techniques have been proposed as solutions to extend performance of conventional electronic ADCs [1]–[5]. The time-stretch technique is one such technique that boosts the performance of an electronic digitizer by slowing down the electrical signal using photonic preprocessing. Conceptually, the time-stretch processing consists of the following three steps.

Step 1) Time-to-wavelength transformation.
Step 2) Wavelength domain processing.
Step 3) Wavelength-to-time mapping.

Time-wavelength mapping occurs when the electrical signal modulates the intensity of a linearly chirped optical pulse. The second and third steps occur simultaneously when this waveform travels through a dispersive optical medium and is subsequently photodetected [2], [6].

The temporal duration of the chirped optical pulse determines the system's time aperture. It has been shown that there is a direct tradeoff between the time aperture and the analog bandwidth, and that the time–bandwidth product (TBP) is an appropriate figure-of-merit for the system [7]. The fundamental limit to TBP is the frequency-dependent phase shift between the upper and lower modulation sidebands caused by optical dispersion. At particular modulation frequencies, this will cause destructive interference between the two sidebands when they beat with the carrier in the photodetector [7]. This RF fading problem is qualitatively similar to the well-known dispersion penalty in analog optical links [8]. Single sideband modulation has been proposed [9] and demonstrated [7] as a means to overcoming the TBP limit set by dispersion penalty. Single sideband modulators rely on microwave hybrid providing quadrature outputs. It is well known that the bandwidth of the hybrid limits the bandwidth over which single sideband modulation can be achieved. Additionally, while single sideband modulation removes the amplitude distortion, it does introduce a phase distortion which must be removed in the digital domain.

In this paper, we proposed a new technique that overcomes the dispersion penalty in a time-stretch ADC. We exploit natural phase diversity that exists between the two outputs of a dual output of a Mach–Zehnder modulator to overcome the RF fading problem caused by dispersion. Experimentally, we demonstrate A/D conversion at 480 Gsample/s with an intrinsic bandwidth of 96 GHz. Additionally, we present the an extension of the maximum ratio combining (MRC) algorithm for application to this system. The MRC will not only eliminate the fading, but will also offer maximum signal-to-noise ratio (SNR). The proposed technique is also applicable to photonic time compression [10] and time reversal [11].

II. PHASE-DIVERSITY TIME-STRETCH PREPROCESSOR

The RF fading phenomenon in the time-stretch system is somewhat similar to the channel fading problem in wireless communication. There, multipath propagation causes interference resulting in spatial fading [12]. In time stretching, frequency fading arises from the interference between two RF sidebands. Spatial diversity, achieved using multiple antennas, has proven to be an effective method to overcome fading in the wireless systems [12]. In the same spirit, the proposed technique makes use of phase diversity, inherent in a dual-output modulator, to overcome the frequency fading in the time-stretch system. In contrast to the wireless system, the fading in time stretch is deterministic, greatly simplifying the system design and signal processing.
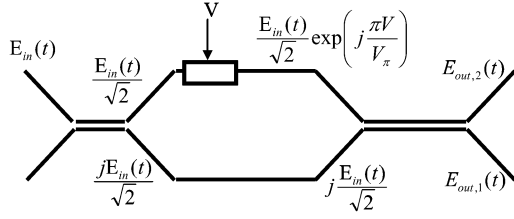
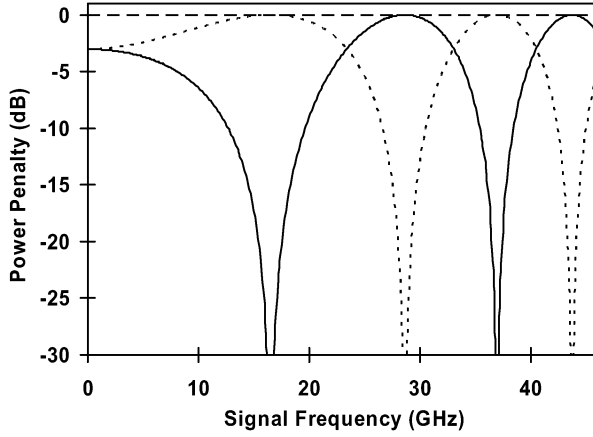Fig. 1.   Signal propagation in a dual-output MZ modulator.

Fig. 2.   Calculated dispersion penalty for two outputs of a single-arm MZ modulator. $H_1(f)$ is shown by the dotted line; $H_2(f)$ is shown by the solid line; $H_1(f) + H_2(f)$ is shown by the the dashed line.
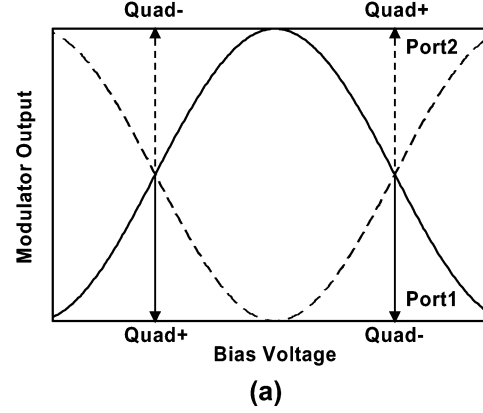

Fig. 3.   Experimental setup of 480-GSa/s phase-diversity photonic time-stretched ADC. SC: supercontinuum; EDFA: erbium-doped fiber amplifier.

Fig. 1 shows a single-arm dual-output Mach–Zehnder (MZ) modulator. The output optical fields $E_{\mathrm{out},1}$ and $E_{\mathrm{out},2}$ are related to the input optical field E_{in} by

$$E_{\mathrm{out},1} = j\frac{E_{\mathrm{in}}}{2}\left(\exp\left(j\frac{\pi V}{V_\pi}\right) + 1\right)$$
$$= jE_{\mathrm{in}}\exp\left(j\frac{\pi V}{2V_\pi}\right)\cos\left(\frac{\pi V}{2V_\pi}\right)$$
$$E_{\mathrm{out},2} = \frac{E_{\mathrm{in}}}{2}\left(\exp\left(j\frac{\pi V}{V_\pi}\right) - 1\right)$$
$$= jE_{\mathrm{in}}\exp\left(j\frac{\pi V}{2V_\pi}\right)\sin\left(\frac{\pi V}{2V_\pi}\right). \qquad (1)$$
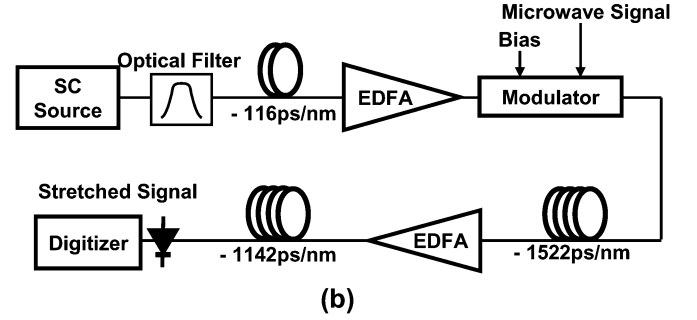
The outputs contain both amplitude and phase modulation. The phase modulation will be converted to amplitude modulation after dispersion in the fiber. The key observation is that the two ports differ by 90° in the phase; hence, their fading characteristics will be different. The RF power spectrum of two outputs is given by [7], [13]

$$H_1(f) = \cos^2\left(\phi_{\mathrm{DIP}} - \frac{\pi}{4}\right) \qquad H_2(f) = \cos^2\left(\phi_{\mathrm{DIP}} + \frac{\pi}{4}\right) \qquad (2)$$

where the dispersion-induced phase (DIP) $\phi_{\mathrm{DIP}} = 2\pi^2\beta_2 L_2 f^2/M$. It depends on the signal frequency f, the length of the second spool of fiber L_2, the fiber group velocity dispersion parameter β_2, and the stretch factor $M = 1 + L_2/L_1$. The plot of power penalty versus the signal frequency is shown in Fig. 2. When one output experiences a null, the other reaches the maximum. This complementary diversity behavior is used to overcome the frequency fading

when both ports are collected. Specifically, $H_1(f) + H_2(f) = \cos^2\left(\phi_{\mathrm{DIP}} - \pi/4\right) + \cos^2\left(\phi_{\mathrm{DIP}} + \pi/4\right) = 1$, free of any fading. We note that both outputs can be stretched in the same fiber and captured by the same digitizer by delaying one by half of the pulse repetition period, and combining them before the stretch fiber. We also note that the phase-diversity time-stretch preprocessor appears similar to the previously published differential time-stretch preprocessor [14]. Both techniques use the dual-output modulator. However, there is a fundamental distinction between the two systems. The differential technique uses the push–pull dual-electrode MZ modulator. Here, the output is pure amplitude modulation with the two ports experiencing the same fading characteristics. In contrast, the phase-diversity technique uses the single-electrode MZ modulator which produces both amplitude and phase modulation.

III. EXPERIMENTS

The experimental setup is shown in Fig. 3. Around 1-ps pulses generated by a passively mode-locked fiber laser at 20 MHz, 1560 nm are used to generate broad-band supercontinuum. By using an optical bandpass filter centered at 1591 nm, ∼15-nm spectrum is sliced for time stretching. The sliced pulse then propagates through a spool of dispersion compensating fiber (DCF) with the total dispersion of $D_1 = -116$ ps/nm, creating a chirped optical pulse with around 1.5-ns time aperture. The sinusoidal signal from an HP83650 synthesizer modulates the chirped pulse using an electrooptic MZ modulator. The dual output modulator in Fig. 1 is emulated by a single-output modulator biased at two different quadrature points, Quad+ and
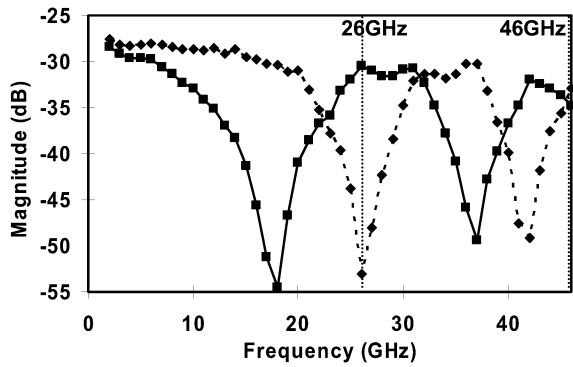
Fig. 4. Measured transfer function of the time-stretch preprocessor. The inherent diversity is demonstrated by the complementary power penalty of two outputs of the modulator.

Quad−. As shown in Fig. 3(a), when biasing at the quadrature point, the two ports of a dual-output modulator are identical to the output of single-port modulators biased at Quad+ or Quad−. The stretch factor is $(D_1 + D_2)/D_1$, where D_1 and D_2 are the total dispersion in the first and second stages, respectively [2], [6]. By using a DCF spool with total dispersion of $D_2 = -2664$ ps/nm, the sinusoid signal is slowed down by ∼24 times. It is then detected by a photodetector and captured by a real-time digital oscilloscope, Tektronix TDS7404 (4-GHz analog bandwidth, 20 GSa/s). The effective sampling rate of the system is 20 GSa/s × 24 = 480 GSa/s and the intrinsic input analog bandwidth is 4 GHz × 24 = 96 GHz. The practical bandwidth is limited by the MZ modulator to approximately 50 GHz. The location and power of EDFAs are chosen to minimize the optical nonlinearities in the fiber while providing a good SNR.

The measured transfer function of the time-stretch system is shown in Fig. 4. The input frequency is swept from 2 to 46 GHz. The figure clearly shows that two ports of modulator experience complementary fading characteristics. The deviation from the ideal behavior shown in Fig. 2 is due to the rolloff in the modulator frequency response and the inaccuracy in bias voltages. The time-domain waveforms at two frequencies marked by the vertical lines in Fig. 4 will be shown next.

The phase diversity between two ports can also be observed in the time domain. To obtain the time-domain waveform, spectral amplitude nonuniformities are removed using the background correction technique described in [13]. The digitized 26-GHz sinusoid signal is shown in Fig. 5 for both outputs. The symbols are digitized samples, and the solid line is sine curve fit. At this frequency, port 1 suffers more than 20-dB power penalty, while the penalty of port 2 is negligible. The measured voltage full-width at half-maximum (FWHM) time aperture is 1.25 ns and the measured stretch factor is 23.95. Using the standard sine fit method, the measured SNR is 32.9 ± 1.25 dB over 200 waveforms, which translates into 5.17 ± 0.21 effective number of bits (ENOB) $\mathrm{ENOB} = (\mathrm{SNR} - 1.76)/6.02$). This SNR is obtained over the full time aperture and 0.4-GHz poststretch bandwidth, which corresponds to 9.6 GHz prestretch bandwidth. A similar measurement at 46 GHz is shown in Fig. 6. At this frequency, port 1 experiences a slightly smaller power penalty than port 2, while both ports maintain a good SNR. The measured SNR at port 1 is 26.7 ± 1.08 dB over 200 waveforms, or 4.14 ± 0.18

Fig. 5. Real-time digitization of a 26-GHz signal. The symbols are digitized samples and the solid line is a sinusoidal fit. (a) Port 1. (b) Port 2.
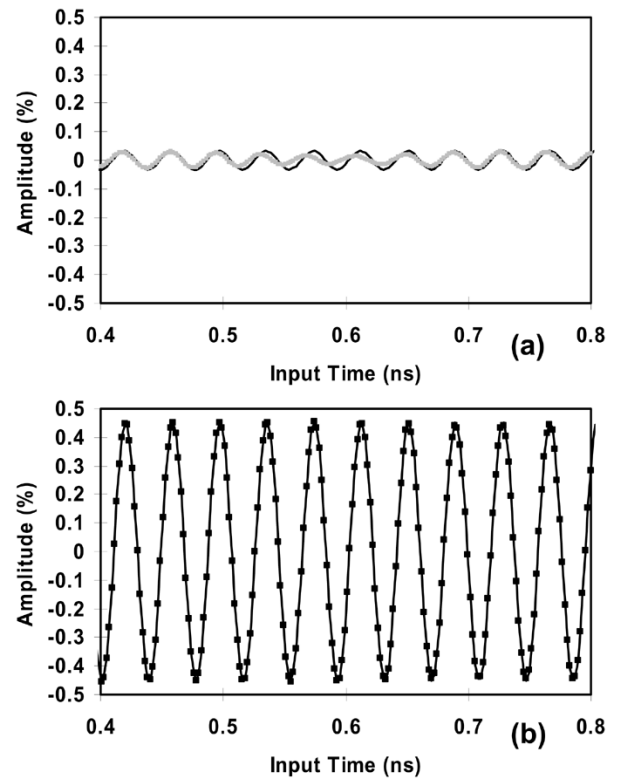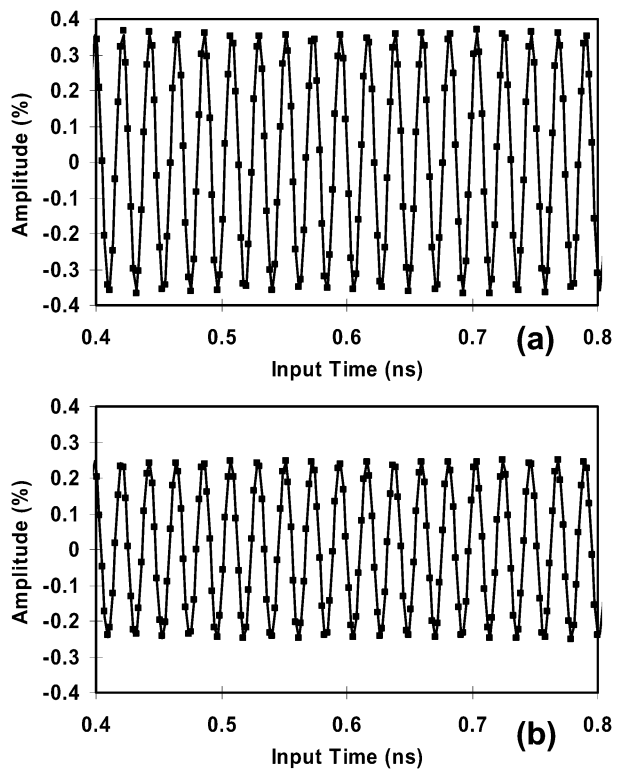

Fig. 6. Real-time digitization of a 46-GHz signal. The symbols are digitized samples and the solid line is a sinusoidal fit. (a) Port 1. (b) Port 2.

ENOB. At port 2, it is 27.5 ± 1.14 dB over 200 pulses, or 4.27 ± 0.19 ENOB. The prestretch bandwidth is 9.6 GHz as well. The time-domain measurements agree well with the results shown

in Fig. 4. By combining the waveforms of two ports, the dispersion penalty can be mitigated. The algorithms are discussed in Section IV.

IV. DISCUSSION

The experimental results presented above clearly demonstrate that the phase-diversity technique can mitigate the dispersion penalty and extend the system analog bandwidth. In principle, single sideband modulation can also mitigate dispersion penalty, however, it introduces phase distortion which must be equalized in the digital domain [7], [9]. Additionally, the bandwidth over which single sideband modulation can be achieved is limited by the microwave hybrid used in the setup.

Due to the similarity between the RF fading in time stretch and the spatial fading in the wireless system, antenna combining algorithms used to maximize the SNR in wireless may also be applicable here. However, there are some differences. In particular, the time stretch is a broad-band (multioctave) and deterministic system while wireless is narrow-band (suboctave) and stochastic. In general, the algorithm used in time stretch will be a broad-band extension of the algorithm used with the wireless system. The fact that the system is deterministic greatly simplifies the problem. A simple solution is to use a switch to select the output having a higher SNR. A more interesting approach is the maximum ratio combining (MRC) algorithm. The MRC algorithm sums the channels with a weight that reflects the voltage SNR in that channel [12]. In time stretch, the weights are $W_1 = \cos(\phi_{\mathrm{DIP}} + \pi/4)$ and $W_2 = \cos(\phi_{\mathrm{DIP}} - \pi/4)$. It can readily be seen that

$$W_1 \cdot \cos\left(\phi_{\mathrm{DIP}} + \left(\frac{\pi}{4}\right)\right) + W_2 \cdot \cos\left(\phi_{\mathrm{DIP}} - \left(\frac{\pi}{4}\right)\right) = 1. \quad (3)$$

Clearly, the weights are proportional to the signal voltage-to-noise ratios. The complementary characteristics of phase diversity ensure that the combined output is independent of frequency as described by (3). In other words, frequency fading is fully eliminated. The broad-band requirement implies that the MRC weights are frequency-dependent, as reflected in the expression for ϕ_{DIP}. The function in (3) is best implemented in the digital domain after A/D conversion. For known fading characteristics, the digital signal processing required for implementation of the MRC algorithm includes two fast Fourier tranform (FFT) transformations, an inverse FFT transformation, and simple multiplication and addition.

The photonic time-stretch system can also perform time compression [10] and time reversal [11] when the two dispersive elements have dispersion parameters with opposite sign. We note that the phase diversity is also applicable to time compression and time reversal since the fading phenomenon is also present in those systems.

By overcoming the dispersion penalty, the phase-diversity technique enables ultrahigh-frequency operation. At very high RF frequencies, other nonideal effects may limit the system performance. The main effects are the frequency-dependent harmonic distortion and distortion due to the nonlinear group velocity dispersion (β_3 of fiber) [13].

Second-order harmonic distortion is clearly visible in Fig. 7, which shows the spectrum of the digitized time-stretched signal
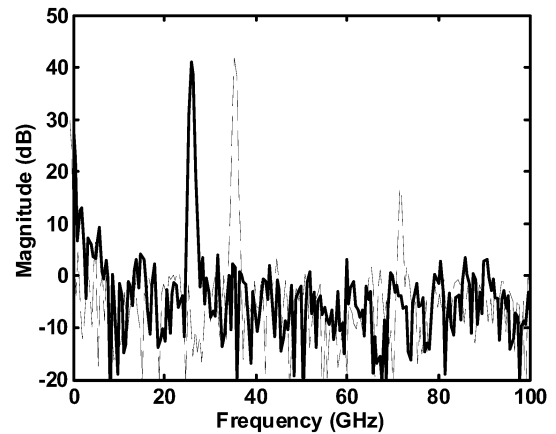

Fig. 7. Digital spectrum of the time-stretch system at 26 GHz (solid line) and 36 GHz (dashed line). These frequencies represent the best and worst cases.

measured at 26 and 36 GHz. These frequencies represent the best and worst cases. A Hanning window is applied before discrete Fourier transform is performed [15]. Since no digital filter is used, the input analog bandwidth in these experiments is 96 GHz (24×4 GHz). At 26 GHz, the second harmonic is below the noise floor, while at 36 GHz the second harmonic is clearly above the noise floor. This frequency-dependent harmonic distortion has been predicted previously [13] and represents memory effect in the system. The phase-diversity technique is based on the linear modulation model and is not able to correct for harmonic distortions. Broad-band linearization techniques [16] in the form of postdistortion performed in the digital domain can potentially be useful.

Another source of distortion at high frequencies is the fiber's nonlinear dispersion, characterized by the β_3 parameter. This introduces a deleterious amplitude modulation across the time aperture [13]. Qualitatively, the existence of β_3 renders the β_2-induced dispersion penalty wavelength-sensitive, and, through wavelength-time mapping, it causes a time-dependent attenuation. In general, a dispersive element with the smaller dispersion slope is desired in the larger bandwidth time-stretch system. Alternatively, the chirped fiber Bragg grating engineered to have zero β_3 can be used, assuming it has sufficient optical bandwidth. In addition, phase diversity can also mitigate this problem. If the deterministic wavelength dependence caused by β_3 is included in the weights in (3), then the MRC algorithm removes the distortion.

V. CONCLUSION

In summary, we have demonstrated a 480-GSa/s photonic ADC with 96-GHz intrinsic bandwidth, using a phase-diversity time-stretch preprocessor. The technique exploits the complimentary RF fading characteristics of the two output ports of an MZ modulator. An effective number of bits of 5.17 is measured over a 9.6-GHz bandwidth centered at a 26-GHz carrier. An extension of the MRC algorithm is proposed as a mean to maximize the SNR. Since the bandwidth is greatly extended by the phase-diversity technique, other effects may limit the system performance. Two such effects, namely the frequency-dependent harmonic distortion and β_3-induced temporal distortion,

are discussed, and possible solutions are proposed. In principle, the phase-diversity and MRC techniques can also be used to eliminate the dispersion penalty in an analog optical link, as well as in photonic time-compression and time-reversal systems.

REFERENCES

[1] M. C. Hamilton and J. A. Bell, "Electro-optical analog-to-digital converter and method for digitizing an analog signal," U.S. Patent 5 010 346, Apr. 23, 1991.

[2] F. Coppinger, A. S. Bhushan, and B. Jalali, "Time magnification of electrical signals using chirped optical pulses," *Electron. Lett.*, vol. 34, no. 4, pp. 399–400, Feb. 1998.

[3] T. R. Clark, J. U. Kang, and R. D. Esman, "Performance of a time- and wavelength-interleaved photonic sampler for analog-digital conversion," *IEEE Photon. Technol. Lett.*, vol. 11, no. 9, pp. 1168–1170, Sep. 1999.

[4] P. W. Juodawlkis, J. C. Twichell, G. E. Betts, J. J. Hargreaves, R. D. Younger, J. L. Wasserman, F. J. O'Donnell, K. G. Ray, and R. C. Williamson, "Optically sampled analog-to-digital converters," *IEEE Trans. Microw. Theory Tech.*, vol. 49, no. 10, pp. 1840–1853, Oct. 2001.

[5] R. Urata, L. Y. Nathawad, K. Ma, R. Takahashi, D. A. B. Miller, B. A. Wooley, and J. S. Harris, Jr, "Ultrafast sampling using low temperature grown GaAs MSM switches integrated with CMOS amplifier for photonic A/D conversion," in *Proc. IEEE LEOS Annu. Meeting*, Glasgow, U.K., Nov. 2002, pp. 809–810.

[6] F. Coppinger, A. S. Bhushan, and B. Jalali, "Photonic time stretch and its application to analog-to-digital conversion," *IEEE Trans. Microw. Theory Tech.*, vol. 47, no. 7, pp. 1309–1314, Jul. 1999.

[7] Y. Han and B. Jalali, "Time-bandwidth product of the photonic time-stretched analog-to-digital converter," *IEEE Trans. Microw. Theory Tech.*, vol. 51, no. 7, pp. 1886–1892, Jul. 2003.

[8] H. Schmuck, "Comparison of optical millimeter-wave system concepts with regard to chromatic dispersion," *Electron. Lett.*, vol. 31, no. 21, pp. 1848–1849, Oct. 1995.

[9] J. M. Fuster, D. Novak, A. Nirmalathas, and J. Marti, "Single-sideband modulation in photonic time-stretch analogue-to-digital conversion," *Electron. Lett.*, vol. 37, no. 1, pp. 67–68, Jan. 2001.

[10] B. Jalali, F. Coppinger, and A. S. Bhushan, "Time-stretch preprocessing overcomes ADC limitations," *Microwave RF Mag.*, vol. 38, no. 3, pp. 57–66, Mar. 1999.

[11] F. Coppinger, A. S. Bhushan, and B. Jalali, "Time reversal of broadband microwave signals," *Electron. Lett.*, vol. 35, no. 15, pp. 1230–1232, Jul. 1999.

[12] T. Rappaport, *Wireless Communications: Principles and Practice*. Englewood Cliffs, NJ: Prentice-Hall, 1996, pp. 177–254.

[13] Y. Han and B. Jalali, "Photonic time-stretched analog-to-Digital converter: Fundamental concepts and practical considerations," *J. Lightwave Technol.*, vol. 21, no. 12, pp. 3085–3103, Dec. 2003.

[14] ——, "Differential photonic time stretch analog-to-digital converter," in *Lasers and Electro-Optics Conf.*, Baltimore, MD, Jun. 2003, pp. 1224–1225.

[15] J. G. Proakis and D. Manolakis, *Digital Signal Processing: Principles, Algorithms and Applications*, 3rd ed. Englewood Cliffs, NJ: Prentice-Hall, 1995.

[16] C. P. Silva, A. A. Moulthrop, M. S. Muha, and C. J. Clark, "Application of polyspectral techniques to nonlinear modeling and compensation," in *IEEE MTT-S Int. Microwave Symp. Dig.*, vol. 1, Phoenix, AZ, May 2001, pp. 13–16.

Yan Han (M'04) received the B.S. and M.S. degrees in electronic engineering from Tsinghua University, Beijing, China, in 1998 and 2000, respectively, and the Ph.D. degree in electrical engineering from the University of California at Los Angeles, in 2004.

He is currently with the College of Optics and Photonics, University of Central Florida, Orlando. He has authored or coauthored over 40 journal publications and conference presentations. His research interests include the areas of time-wavelength, ultrawide-band signal processing, advanced modulation formats for optical communications, microwave photonics, optical amplification, and nonlinear optics.

Ozdal Boyraz received the B.S. degree in electrical engineering from Hacettepe University, Ankara, Turkey, in 1993, and the M.S. and Ph.D. degrees from The University of Michigan at Ann Arbor, in 1997 and 2001, respectively.

He is currently a Post-Doctoral Research Fellow with the University of California at Los Angeles. He has authored or coauthored over 40 publications. He holds three U.S. patents. His research areas include nonlinear optics, silicon photonics, microwave photonics, fiber-optical communication systems, and integrated optics.

Bahram Jalali (S'86–M'89–SM'97–F'04) is currently a Professor of Electrical Engineering, the Director of the Defense Advanced Research Projects Agency (DARPA) Center for Optical A/D System Technology (COAST), and the Director of the Optoelectronic Circuits and System Laboratory, University of California at Los Angeles (UCLA). From 1988 to 1992, he was a Member of the Technical Staff with the Physics Research Division, AT&T Bell Laboratories, Murray Hill, NJ, where he conducted research on ultrafast electronics and optoelectronics. He was responsible for the successful development and delivery of 10-Gb/s lightwave circuits to the U.S. Air Force in 1992. From 1999 to 2001, while on leave from UCLA, he founded Cognet Microsystems, a Los Angeles-based fiber-optic component company that was acquired by the Intel Corporation in 2001. He currently serves as a consultant for the Wireless Networking Group (WNG) of the Intel Corporation and serves on the Board of Trustees of the California Science Center. He has authored or coauthored over 120 publications. He holds five U.S. patents. His current research interests are microwave photonics, integrated optics, and fiber-optic integrated circuits.

Dr. Jalali is a member of the California Nano Sciences Institute (CNSI) and is the chair of the Los Angeles Chapter of the IEEE Lasers and Electro-Optics Society (LEOS). He was the general chair for the 2001 IEEE International Conference on Microwave Photonics (MWP) and its Steering Committee chair (2001–present). He was the recipient of the BridgeGate 20 Award in recognition of his contributions to the Southern California hi-tech economy.